Inorg. Chem. **2004**, *43*, 5931–5943

Intra and Intermolecular Magnetic Interactions in a Series of Dinuclear Cu(II)/hxta Complexes {H_5hxta = *N*,*N*′-(2-hydroxy-1,3-xylylene)-bis-(*N*-carboxymethylglycine)}: Correlation of Magnetic Properties with Geometry

Steve Laborda,[†] Rodolphe Clérac,[‡] Christopher E. Anson,[†] and Annie K. Powell*,[†]

Institut für Anorganische Chemie, Universität Karlsruhe, Engesserstrasse Geb. 30.45, D-76128 Karlsruhe, Germany, and Centre de Recherche Paul Pascal, CNRS UPR 8641, 115 Avenue Dr. A. Schweitzer, 33600 Pessac, France

Received November 18, 2003

Nine dinuclear copper(II) complexes with hxta^{5-} ligands {H_5hxta = *N*,*N*′-(2-hydroxy-1,3-xylylene)-bis-(*N*-carboxymethylglycine)}: $[Cu_2(MeO\text{-}hxtaH)(H_2O)_2]\cdot 4H_2O$ (**1**), $[Na(\mu\text{-}H_2O)_2(H_2O)_6][Cu_2(Cl\text{-}hxta)(H_2O)_3]_2\cdot 6H_2O$ (**2**), $[Cu(H_2O)_6][Cu_2(Me\text{-}hxta)(H_2O)_2](NO_3)\cdot 2H_2O$ **(3)**, $[Cu_2(R\text{-}hxtaH)(H_2O)_3]\cdot 3H_2O$ {R = Cl (**4**), CH_3 (**5**), and MeO (**6**)}, $[Cu_2(MeO\text{-}hxtaH_2)(\mu\text{-}X)(CH_3OH)]\cdot 3CH_3OH$ {X = Cl (**7**), Br (**8**)} and $K_5Na(\mu\text{-}H_2O)_{10}[Cu_2(\mu\text{-}CO_3)(Me\text{-}hxta)]_2\cdot 4H_2O$ (**9**), have been synthesized and structurally characterized. In complexes **4**–**7**, the dinuclear units are linked via novel pairwise supramolecular interactions involving the ligand carboxylate groups. The intra- and intermolecular magnetic interactions have been quantified, and the coupling constants have been related to the structural geometries.

Introduction

Over the past twenty years or so, research into molecular-based magnetism has become well established with an underlying theme of aiming to produce usable devices based on this technology. To achieve this goal it is necessary to learn how to direct certain favorable structural motifs which lead to magnetic ordering over useful temperature regimes, and much fundamental research into what Kahn[1] termed "magnetic bricks" which can be combined to give an ordered solid is also necessary. An important concept in achieving a functional material based on molecular motifs is the creation of a solid with a variety of coupling regimes which come into play at different temperatures allowing for thermal switching of states for a specific application. We have previously discussed this idea of combining strong and weaker couplings in one coordination solid to produce a rich magnetic phase diagram which, in turn, offers a means for moving between various magnetic regimes.[2,3] Here we report on the quantification of magnetic coupling within a series of closely related dinuclear Cu^{II} compounds which can serve as the bricks to build up such materials.

Although much work has been done on dinuclear copper(II) based systems in the past, these have tended to be fairly simple motifs containing $\{Cu(\mu\text{-}X)_2Cu\}$ structural elements where the magnetic coupling has been correlated with Cu···Cu distances and Cu−X−Cu angles.[4−7] The degree of magnetic coupling between two Cu^{II} centers is related to a number of parameters which can be determined using single-crystal X-ray analyses. The pathway for coupling is the available orbital interactions between copper centers provided by the way in which the bridging species arrange the local copper geometries. The especially flexible nature of the copper(II) coordination sphere plays a vital role here assisted by the Jahn−Teller effect which can be realized either by distortion of an octahedral geometry to give a 4 + 2 bonding

* Author to whom correspondence should be addressed. E-mail: powell@chemie.uni-karlsruhe.de. Fax: +49 721 608 8142. Telephone: +49 721 608 2135.
[†] Universität Karlsruhe.
[‡] Centre de Recherche Paul Pascal.

(1) Kahn, O. *Molecular Magnetism*; VCH: New York, 1993.
(2) Murugesu, M.; Clérac, R.; Pilawa, B.; Mandel, A.; Anson, C. E.; Powell, A. K. *Inorg. Chim. Acta* **2002**, *337*, 328−336.
(3) King, P.; Clérac, R.; Anson, C. E.; Coulon, C.; Powell, A. K. *Inorg. Chem.* **2003**, *42*, 3492−3500.
(4) Charlot, M. F.; Jeannin, S.; Kahn, O.; Lucrece-Abaul, J.; Martin-Frere, J. *Inorg. Chem.* **1979**, *18*, 1675−1681.
(5) Crawford, V. H.; Richardson, H. W.; Wasson, J. R.; Hodgson, D. J.; Hatfield, W. E. *Inorg. Chem.* **1976**, *15*, 2107.
(6) Thompson, L. K.; Mandal, S. K.; Tandon, S. S.; Bridson, J. N.; Park, M. K. *Inorg. Chem.* **1996**, *35*, 3117−3125.
(7) Merz, L.; Haase, W. J. *J. Chem. Soc., Dalton Trans.* **1980**, 875.

10.1021/ic035333m CCC: $27.50 © 2004 American Chemical Society
Published on Web 08/20/2004

situation or else by a change in coordination number as an alternative means of lifting the degeneracy of unequally occupied d-orbitals. The most usually encountered situations are penta-coordination with the extremes of trigonal bipyramidal and square-based pyramidal geometry. Since the orbital splitting diagrams for all of these arrangements lead to different possibilities for overlap of "magnetic orbitals" it is necessary to consider the geometric parameters of copper(II) coordination geometry, Cu(II)···Cu(II) separation and Cu−X−Cu angle, which we define as α, to correlate structural and magnetic properties for these "magnetic bricks".

Concerning coordination geometry, for the 4 + 2 geometry two situations are possible. If the ligands along the *z*-axis are further away from the copper(II) center than those in the *xy* plane, then we expect the $d_{x^2-y^2}$ orbital to be singly occupied and highest in energy, which is termed the $d_{x^2-y^2}$ ground state. For the case where the geometry is axially compressed along *z* then the converse will occur and now the d_{z^2} orbital will be higher and singly occupied, which is known as the d_{z^2} ground state. For the two extremes of penta-coordination, in the square-pyramidal geometry, if one of the ligands along the *z*-axis is removed, then we expect the $d_{x^2-y^2}$ orbital to be singly occupied and highest in energy, and on the contrary in a trigonal bipyramidal environment, if one ligand in the *xy* plane is removed the d_{z^2} orbital will be higher and singly occupied.

For the situation where the bridging species that mediate the magnetic coupling are different, no attempt has been made to correlate coupling with geometric parameters, largely because of a lack of suitable comparative structures containing the {Cu(*μ*-X)(*μ*-Y)Cu} motif. Similarly, there are few structures in the literature of dinuclear Cu(II) complexes in which the copper centers are linked by a single bridging atom.[8−14] In this paper we report on the structures and magnetic behavior of compounds with dinuclear copper(II) motifs {Cu(*μ*-hxta)Cu} where the bridging between the metal centers is provided by the oxygen of a single phenoxy bridge from a $(R\text{-hxta})^{5-}$ ligand (H_5hxta = *N*,*N*′-(2-hydroxy-1,3-xylylene)-bis-(*N*-carboxymethylglycine); R = Cl, Me, MeO, Scheme 1) and {Cu(*μ*-hxta)(*μ*-X)Cu} in which the coppers are linked both by the phenoxy bridge as well as a chloro, bromo, or carbonato bridging ligand. Since magnetostructural investigations for such bridging motifs are seldom found in the literature we felt it would be useful to explore the trends in magnetic coupling in such systems.

The strength of the magnetic interaction in a dinuclear Cu(II) complex is not only dependent on the nature and geometry of the bridge between them. The nature of the peripheral ligands can also have a significant effect, and for phenoxy bridges the degree of twisting of the aromatic ring relative to the Cu_2O plane is also important.[15−17] To study any correlation between *J* and the bridge geometry it is thus necessary to at least minimize these potential complications.

Scheme 1

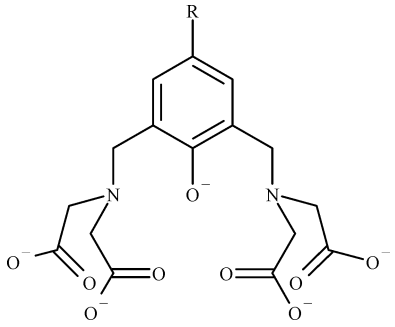

The $(R\text{-hxta})^{5-}$ ligands were selected in this work, since related ligands have already shown their ability to form binuclear Cu(II) complexes.[12,13,17−23] They provide a convenient dinucleating feature with the phenolate oxygen providing the bridging function, and the $RN(CH_2COOH)_2$ arms, which are derived from the well-known iminodiacetic acid ligand, adopting a chelating function. The coordination sphere around the Cu(II) centers will thus always consist of the phenoxy bridge, an amino nitrogen atom, and two carboxylate oxygens, with the possibility for just one or two further monodentate ligands, many of which will be water or methanol molecules. Furthermore, the steric demands of the $(R\text{-hxta})^{5-}$ ligands will be similar from complex to complex, minimizing the variation in the out-of-plane twisting of the phenoxy ring. Complexes of such ligands would thus be well-suited to an investigation of the variation of the magnetic interaction with changes in the geometry at the bridging phenoxo-oxygen, as variation in all other geometric factors that can influence the interaction are minimized.

The presence of carboxylate groups in these ligands can also offer the possibility of further *extra*-dimer carboxylate bridging and so allow the creation of supramolecular structures involving these binuclear complexes as a "magnetic brick". Furthermore, efforts to create supramolecular aggregates of paramagnetic transition metal clusters can be helped by the hydrophilic and hydrophobic regions of the

(8) Berends, H. P.; Stephan, D. W. *Inorg. Chem.* **1987**, *26*, 749−754.
(9) Nishida, Y.; Shimo, H.; Maehara, H.; Kida, S. *J. Chem. Soc., Dalton Trans.* **1985**, 1945−1951.
(10) Oberhausen, K. J.; Richardson, J. F.; Buchanan, R. M.; McCusker, J. K.; Hendrickson, D. N.; Latour, J. M. *Inorg. Chem.* **1991**, *30*, 1357−1365.
(11) Torelli, S.; Belle, C.; Gautier-Luneau, L.; Pierre, J. L.; Saint-Aman, E.; Latour, J. M.; Pape, L. L.; Luneau, D. *Inorg. Chem.* **2000**, *39*, 3526−3536.
(12) Koval, I. A.; Pursche, D.; Stassen, A. F.; Gamez, P.; Krebs, B.; Reedijk, J. *Eur. J. Chem.* **2003**, 1669−1674.
(13) Berends, H. P.; Stephan, D. W. *Inorg. Chim. Acta* **1985**, *99*, L53−L56.
(14) Berends, H. P.; Stephan, D. W. *Inorg. Chem.* **1987**, *26*, 749−754.
(15) Ruiz, E.; Alemany, P.; Alvarez, S.; Cano, J. *J. Am. Chem. Soc.* **1997**, *119*, 1297−1303.
(16) Ruiz, E.; Alemany, P.; Alvarez, S.; Cano, J. *Inorg. Chem.* **1997**, *36*, 3683−3688.
(17) Choudhury, C. R.; Dey, S. K.; Karmakar, R.; Wu, C.-D.; Lu, C.-Z.; Fallah, M. S. E.; Mitra, S. *New J. Chem.* **2003**, *27*, 1360−1366.
(18) Holz, R. C.; Brink, J. M.; Gobena, F. T.; O'Connor, C. J. *Inorg. Chem.* **1994**, *33*, 6086−6092.
(19) Brink, J. M.; Rose, R. A.; Holz, R. C. *Inorg. Chem.* **1996**, *35*, 2878−2885.
(20) Holz, R. C.; Bennett, B.; Chen, G.; Ming, L. *J. Am. Chem. Soc.* **1998**, *120*, 6329−6335.
(21) Holz, R. C.; Bradshaw, J. M.; Bennett, B. *Inorg. Chem.* **1998**, *37*, 1219−1225.
(22) Branum, M. E.; Tipton, A. K.; Zhu, S.; Que, L., Jr. *J. Am. Chem. Soc.* **2001**, *123*, 1898−1904.
(23) Nishida, Y.; Nasu, M.; Yamada, K. *Chem. Lett.* **1990**, 195−198.

Table 1. Crystallographic Data and Details of Structure Determinations for Complexes **1**−**3**

compound	**1**	**2**	**3**
formula	$C_{17}H_{30}Cu_2N_2O_{16}$	$C_{32}H_{64}Cl_2Cu_4N_4Na_2O_{36}$	$C_{17}H_{37}Cu_3N_3O_{22}$
formula weight	645.51	1451.91	826.12
crystal system	monoclinic	monoclinic	triclinic
space group	$P2_1/c$	$P2_1/n$	$P\bar{1}$
a (Å)	13.6420(9)	9.7480(3)	10.9861(10)
b (Å)	11.8818(8)	17.9786(6)	11.9354(11)
c (Å)	15.8709(11)	15.7561(5)	12.2807(11)
			69.841(10)
β (deg)	108.893(8)	98.777(1)	89.940(10)
			80.984(11)
V (Å^3)	2433.9(3)	2729.00(15)	1490.5(2)
Z	4	2	2
temperature (K)	200	200	200
F(000)	1328	1488	846
d_{calc} (mg m^{-3})	1.762	1.767	1.841
μ(Mo Kα) (mm^{-1})	1.830	1.756	2.218
crystal size (mm)	0.40 × 0.30 × 0.10	0.11 × 0.06 × 0.03	0.18 × 0.15 × 0.12
diffractometer	Stoe IPDS	Bruker SMART Apex	Stoe IPDS
data measured	15710	13553	9924
unique data	4815	6040	5505
R_{int}	0.0717	0.0497	0.0409
data with $I \geq 2\sigma(I)$	2547	5399	4271
parameters	387	434	467
wR_2, R_1 (all data)	0.1201, 0.0605	0.1017, 0.0428	0.1373, 0.0640
wR_2, R_1 [$I \geq 2\sigma(I)$]	0.1154, 0.0474	0.0984, 0.0381	0.1338, 0.0551
S (all data)	0.902	1.085	0.971
biggest diff. peak, hole (eÅ^{-3})	+1.29, −0.51	+0.46, −0.74	+1.26, −0.48

ligands.[24,25] This will be discussed in a further publication. However, for the reasons just discussed, the structural correlations for the *intra*-dimer magnetic interactions obtained in this work should still be valid when the dinuclear complex bricks are built into more complex structures, and so facilitate the interpretation of the magnetic behavior of the more complicated systems.

Experimental Section

All starting materials were commercial products and were used as supplied. Elemental analyses were obtained at the Institut für Anorganische Chemie, University of Karlsruhe. IR spectra were recorded on a Perkin-Elmer Spectrum One FTIR spectrometer with 16 scans and a resolution of 4 cm^{-1} using KBr pellets.

Syntheses. The ligands of general formula Na_3(R-hxtaH_2) where R = Cl, CH_3 and CH_3O were prepared according to the procedure of Murch et al.[26]

Caution: It has been reported that Na_3(CH_3-hxtaH_2) can cause allergic reactions.

[Cu_2(MeO-hxtaH)(H_2O)$_2$]·4H_2O (1). $Cu(NO_3)_2$·6H_2O (120 mg, 0.50 mmol) was dissolved in water (5 mL). An aqueous solution (10 mL) of Na_3(CH_3O-hxtaH_2) (100 mg, 0.25 mmol) and $NaOCH_3$ (6.8 mg, 0.125 mmol) was added dropwise. The mixture was allowed to stand at room-temperature overnight and 93 mg (yield: 56%; based on ligand) of green crystals was obtained. Anal. Calcd for $C_{17}H_{30}Cu_2N_8O_{16}$: C, 31.60; H, 4.65; N, 4,65. Found: C, 31.45; H, 4.66; N, 4.33. IR (cm^{-1}): 1660 (vs), 1623 (vs), 1599 (vs), 1471-(s), 1440 (s), 1397(s), 1352 (m), 1321 (s), 1297 (m), 1261 (s), 1228 (w).

[Na_2(μ-H_2O)$_2$(H_2O)$_6$][Cu_2(Cl-hxta)(H_2O)$_3$]$_2$·6H_2O (2). Na_3(Cl-hxtaH_2) (100 mg, 0.25 mmol) and $NaOCH_3$ (108 mg, 2.0 mmol) were dissolved in 10 mL of water and added to an aqueous solution (5 mL) of $Cu(NO_3)_2$·6H_2O (120 mg, 0.50 mmol). After the mixture stood for several hours at room temperature, green parallelopiped crystals were isolated with a yield of 19% (72 mg) (based on ligand). Anal. Calcd for $C_{32}H_{64}Cl_2Cu_4N_4Na_2O_{36}$: C, 26.47; H, 4.44; N, 3.85. Found: C, 26.64; H, 4.38; N, 3.71. IR (cm^{-1}): 1618 (vs), 1492 (w), 1461 (m), 1441 (m), 1435 (m), 1426 (m), 1395 (s), 1367 (m), 1358 (m), 1328 (m), 1315 (m), 1296 (m), 1285 (m), 1266 (w), 1251 (m), 1234 (w).

[$Cu(OH_2)_6$][Cu_2(MeO-hxtaH)(H_2O)$_2$](NO_3)·2H_2O (3). Na_3(Me-hxtaH_2) (100 mg, 0.25 mmol) and KOH (98 mg, 1.75 mmol) were dissolved in 20 mL of water and added to a stirred methanolic solution (5 mL) of $Cu(NO_3)_2$·6H_2O (120 mg, 0.50 mmol). After the mixture stood for several hours at room temperature, green parallelopiped crystals were isolated with a yield of 60% (134 mg) (based on the ligand). Anal. Calcd for $C_{17}H_{31}Cu_3N_3O_{19}$: (corresponding to loss of 3 H_2O) C, 26.47; H, 4.05; N, 5.44. Found: C, 26.59; H, 3.55; N, 5.15. IR (cm^{-1}): 1598 (vs), 1476 (m), 1384 (s), 1337 (m), 1320 (m), 1307 (m), 1275 (m), 1249 (m).

[Cu_2(R-hxtaH)(H_2O)$_3$]·3H_2O {R = Cl (4), CH_3 (5), and CH_3O (6)}. Na_3(R-hxtaH_2) (0.25 mmol) was dissolved in 10 mL of water and added to a stirred aqueous solution (5 mL) of $Cu(NO_3)_2$·6H_2O (120 mg, 0.50 mmol). After a few hours and slow evaporation of the solvent, green parallelopiped crystals were isolated by filtration in a yield of 70% (based on ligand). **(4)** Anal. Calcd for $C_{17}H_{27}Cu_2N_2O_{15}Cl$: C, 29.54; H, 4.15; N, 4.42. Found: C, 29.80; H, 4.18; N, 4.42. IR (cm^{-1}): 1618 (vs), 1462 (s), 1434 (m), 1397 (s), 1324 (m), 1306 (m),1283 (w),1250 (m). **(5)** Anal. Calcd for $C_{17}H_{30}Cu_2N_2O_{15}$: C, 32.41; H, 4.76; N, 4.76. Found: C, 32.56; H, 4.72; N, 4.48. IR (cm^{-1}): 1618 (vs), 1581(s), 1475(s), 1422 (m), 1393 (s), 1316 (w), 1303 (w), 1272 (w), 1240 (w). **(6)** Anal. Calcd for $C_{17}H_{30}Cu_2N_2O_{16}$: C, 31.60; H, 4.65; N, 4.65. Found: C, 31.65; H, 4.67; N, 4.52. IR (cm^{-1}): 1618 (vs), 1470 (s), 1436 (m), 1390 (s), 1323 (m), 1305 (m), 1268 (s), 1239 (w).

[Cu_2(CH_3O-hxtaH$_2$)(X)(CH_3OH)]·3CH_3OH {X = Cl (7), Br (8)}. A methanol solution (30 mL) of Na_3(CH_3O-hxtaH_2) (100 mg, 0.25 mmol) was added to a methanolic solution (10 mL) of

(24) Schmitt, W.; Murugesu, M.; Goodwin, J. C.; Hill, J. P.; Mandel, A.; Bhalla, R.; Anson, C. E.; Heath, S. L.; Powell, A. K. *Polyhedron* **2001**, *20*, 1687−1697.
(25) Geetha, K.; Nethaji, M.; Chakravarty, A. R. *Inorg. Chem.* **1997**, *36*, 6134−6137.
(26) Murch, B. P.; Bradley, F. C.; Papaefthymiou, B. P. D.; Que, L., Jr. *J. Am. Chem. Soc.* **1987**, *109*, 7993−8003.

Table 2. Crystallographic Data and Details of Structure Determinations for Complexes **4**−**6**

compound	**4**	**5**	**6**
formula	$C_{16}H_{27}ClCu_2N_2O_{15}$	$C_{17}H_{30}Cu_2N_2O_{15}$	$C_{17}H_{30}Cu_2N_2O_{16}$
formula weight	649.93	629.51	645.51
crystal system	monoclinic	monoclinic	monoclinic
space group	$P2_1/n$	$P2_1/n$	$P2_1/n$
a (Å)	14.9546(14)	15.0808(12)	14.8149(12)
b (Å)	10.7600(7)	10.8279(6)	11.1467(6)
c (Å)	15.2001(11)	15.1972(11)	15.1721(11)
α (deg)			
β (deg)	105.198(10)	104.659(9)	105.544(9)
γ (deg)			
V (Å^3)	2360.3(3)	2400.8(3)	2413.8(3)
Z	4	4	4
temperature (K)	200	200	200
F(000)	1328	1296	1328
d_{calc} (mg m^{-3})	1.829	1.742	1.776
μ(Mo Kα) (mm^{-1})	1.994	1.850	1.845
crystal size (mm)	0.30 × 0.25 × 0.15	0.25 × 0.25 × 0.20	0.25 × 0.20 × 0.15
diffractometer	Stoe IPDS	Stoe IPDS	Stoe IPDS
data measured	9300	13006	12357
unique data	4485	4440	4517
R_{int}	0.0626	0.0560	0.0722
data with $I \geq 2\sigma(I)$	3427	3282	3172
parameters	432	445	454
wR_2, R_1 (all data)	0.1238, 0.0591	0.0918, 0.0497	0.0925, 0.0542
wR_2, R_1 [$I \geq 2\sigma(I)$]	0.1177, 0.0466	0.0876, 0.0363	0.0878, 0.0375
S (all data)	0.937	0.893	0.885
biggest diff. peak, hole (e Å^{-3})	+0.98, −0.73	+0.46, −0.34	+0.58, −0.52

Table 3. Crystallographic Data and Details of Structure Determinations for Complexes **7**−**9**

compound	**7**	**8**	**9**
formula	$C_{22}H_{39}ClCu_2N_2O_{15}$	$C_{22}H_{39}BrCu_2N_2O_{15}$	$C_{36}H_{62}Cu_4K_5N_4NaO_{38}$
formula weight	734.08	778.54	1631.55
crystal system	monoclinic	monoclinic	monoclinic
space group	$P2_1/n$	$P2_1/n$	$P2_1/c$
a (Å)	10.8585	10.9594(5)	16.9553(18)
b (Å)	12.0613	12.1146(6)	7.8694(8)
c (Å)	23.2112(15)	23.9460(10)	22.512(2)
α (deg)			
β (deg)	94.118(8)	93.946(1)	106.335(2)
γ (deg)			
V (Å^3)	3032.1(3)	3080.6(3)	2882.4(5)
Z	4	4	2
temperature (K)	200	200	200
F(000)	1520	1592	1664
d_{calc} (mg m^{-3})	1.608	1.679	1.880
μ(Mo Kα) (mm^{-1})	1.562	2.748	1.933
crystal size (mm)	0.30 × 0.15 × 0.10	0.20 × 0.10 × 0.05	0.40 × 0.25 × 0.05
diffractometer	Stoe IPDS	Bruker SMART Apex	Bruker SMART Apex
data measured	18308	15236	10598
unique data	5940	6841	5765
R_{int}	0.0838	0.0446	0.0343
data with $I \geq 2\sigma(I)$	3548	5574	4895
parameters	442	405	414
wR_2, R_1 (all data)	0.1083, 0.0787	0.1099, 0.0514	0.2191, 0.0838
wR_2, R_1 [$I \geq 2\sigma(I)$]	0.0985, 0.0438	0.1056, 0.0410	0.2124, 0.0754
S (all data)	0.832	1.050	1.035
biggest diff. peak, hole (e Å^{-3})	+0.77, −0.37	+1.09, −0.68	+2.69, −1.54

$CuX_2 \cdot 6H_2O$ (X = Cl, Br) (1.0 mmol). After several days, dark brown-green crystals were obtained by slow evaporation with a yield of 20% (based on the ligand). Crystals of **7** and **8** readily lose solvent, so it was not possible to obtain accurate microanalytical data, and IR spectra were of poor quality.

$[K_5Na(\mu\text{-}H_2O)_{10}][Cu_2(\mu\text{-}CO_3)(Me\text{-}hxta)]_2 \cdot 4H_2O$ (9). $CuCl_2 \cdot 6H_2O$ (85 mg, 0.50 mmol) was dissolved in water (5 mL). An aqueous solution (10 mL) of $Na_3(CH_3O\text{-}hxtaH_2)$ (100 mg, 0.25 mmol) and KOH (70 mg, 1.25 mmol) was added dropwise. Yellow-green needles were obtained on standing at room temperature for two weeks, with a yield of 22% (based on ligand). Anal. Calcd for $C_{36}H_{62}Cu_4K_5NaN_4O_{38}$: C, 26.50; H, 3.83; N, 3.43. Found: C, 26.40; H, 3.70; N, 3.20. IR (cm^{-1}): 1619 (vs), 1548 (s), 1477 (m), 1455 (w), 1393 (s), 1334 (s), 1280 (m), 1249 (m).

Magnetic Measurements. The magnetic susceptibility measurements were obtained with the use of a Quantum Design SQUID magnetometer MPMS-XL. Measurements were performed on finely ground crystalline samples of **1** (26.57 mg), **2** (20.30 mg), **3** (9.92 mg), **4** (43.60 mg), **5** (26.59 mg), **6** (32.10 mg), **7** (21.28 mg), **8** (31.11 mg), and **9** (17.82 mg). Magnetic data were corrected for the sample holder and the diamagnetic contribution from Pascal's constants.[27]

X-ray Data Collection and Crystal Structure Determination. Data were measured on a Stoe IPDS image plate area detector

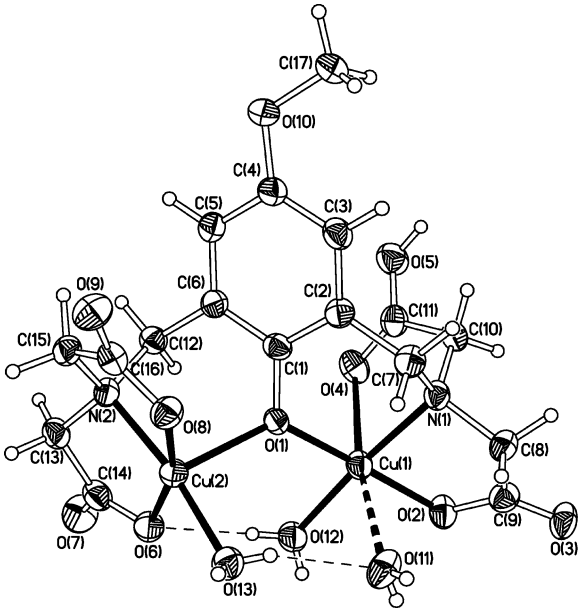

Figure 1. Representation of the dinuclear unit in $[Cu_2(MeO\text{-}hxtaH)(H_2O)_2]\cdot 4H_2O$, **1**.

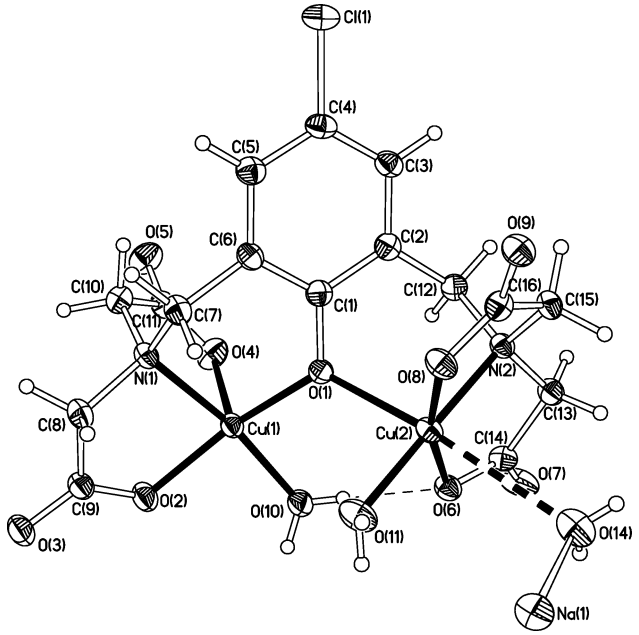

Figure 2. Dinuclear complex in $[Na_2(\mu\text{-}H_2O)_2(H_2O)_6][Cu_2(Cl\text{-}hxta)(H_2O)_3]_2\cdot 6H_2O$, **2**.

diffractometer or a Bruker SMART Apex CCD diffractometer (see Tables 1−3), both using graphite-monochromated Mo Kα radiation (λ = 0.71073 Å). The data for **2**, **7**, and **8** were corrected for absorption using the program SADABS.[28] Structures were solved by direct methods and refined by full-matrix least-squares against F^2 (all data) using the SHELXTL software package.[29] Non-hydrogen atoms were assigned anisotropic thermal parameters. Hydrogen atoms bonded to oxygen were located and fully refined with isotropic temperature factors, except in **8**, where hydrogens of bridging waters were placed in idealized positions. In the structures of **3**, **4**, and **5** the methylene and aromatic hydrogens of the hxta ligands were fully refined, otherwise they were placed in idealized positions. Crystals of **9** usually showed signs of twinning; this may explain the higher than expected peaks in the final difference maps. Crystal data and data collection details are summarized in Tables 1−3. Crystallographic data (excluding structure factors) for the structures in this paper have been deposited with the Cambridge Crystallographic Data Centre as supplementary publication nos. CCDC 224422−224430. Copies of the data can be obtained, free of charge, on application to CCDC, 12 Union Road, Cambridge CB2 1EZ, UK; http://www.ccdc.cam.ac.uk/perl/catreq/catreq.cgi; data_request@ccdc.cam.ac.uk; or fax +44 1223 336033.

Results and Discussion

The ligand $Na_3(R\text{-}hxtaH_2)$ in the presence of $Cu(NO_3)_2\cdot 6H_2O$ with 0.5 equivalent of sodium methoxide forms compound **1**, and with 8 equivalents forms compound **2**.

$[Cu_2(MeO\text{-}hxtaH)(H_2O)_2]\cdot 4H_2O$, **1**, is a mono-phenoxy-bridged dinuclear copper(II) complex (Figure 1). The phenoxy oxygen O(1) forms an unsymmetrical bridge between the two copper centers Cu(1) and Cu(2) (Cu(1)−O(1) = 1.911(2) Å, Cu(2)−O(1) = 2.174(2) Å, Cu(1)−O(1)−Cu(2) = 130.9(1)°), with a Cu(1)···Cu(2) separation of 3.7172(6) Å. The coordination geometry about Cu(1) is between a (4 + 1 + 1) distorted octahedral and a (4 + 1) square-pyramidal environment. The two axial positions of the octahedral geometry are occupied by the carboxylate oxygen O(4) and an only weakly coordinated water molecule O(11) (Cu(1)−O(4) = 2.393(4) Å, Cu(1)−O(11) = 2.864(3) Å). The four equatorial positions are occupied by the phenoxy oxygen O(1), N(1) and O(2) of the ligand arm, and an aqua ligand O(12). The geometry about Cu(2) is square-based pyramidal, with an amine nitrogen and two carboxylate oxygens from the hxta ligand, and an aqua ligand (O(13)) in the equatorial plane and O(1) in the apical position. The aromatic ring of the ligand is twisted relative to the Cu(1)−O(1)−Cu(2) plane with a dihedral angle of 46.7°. One of the outer, or noncoordinated, carboxylate oxygens, O(5), is protonated, resulting in a neutral complex. The aqua ligand O(12) forms a strong *intra*-molecular hydrogen bond to carboxylate oxygen O(6), while dimers are linked by pairwise *inter*-dimer hydrogen bonding from O(13) to O(9) of the inversion-related complex at $\{-x + 1, -y + 1, -z\}$.

The dinuclear copper(II) complex in $[Cu_2(Cl\text{-}hxta)(H_2O)_3]_2[Na(\mu\text{-}H_2O)_2(H_2O)_6]\cdot 6H_2O$, **2**, is shown in Figure 2, and is structurally similar to that in **1**. Again, the phenoxy bridge is unsymmetrical, with Cu(1)−O(1) 1.917(2) Å, Cu(2)−O(1) 2.225(2) Å, and the Cu(1)−O(1)−Cu(2) angle 126.01(8)°; the Cu(1)···Cu(2) separation is 3.6933(4) Å. The environment about Cu(1) is square-based pyramidal. The apical site is occupied by the carboxylate oxygen O(4), while the equatorial plane is defined by the phenoxy oxygen O(1), the carboxylate oxygen O(2), the amino nitrogen N(1), and an aqua ligand O(11). Cu(2) has a geometry similar to that of compound **1**. Again, the equatorial plane is described by the amine nitrogen and two carboxylate oxygens from an arm of the ligand, together with an aqua ligand O(11), while O(1) is in an axial site. However, in **2** the octahedral coordination sphere about Cu(2) is now completed by a weak interaction

(27) Boudreaux, E. A.; Mulay, L. N. *Theory and Applications of Molecular Paramagnetism*; Wiley: New York, 1976.
(28) Sheldrick, G. M. *SADABS (The Siemens Area Dectector Absorption Correction)*; Bruker AXS Inc.: Madison, WI, 1996.
(29) Sheldrick, G. M. *SHELXTL 5.1*; Bruker AXS Inc.: Madison, WI, 1997.

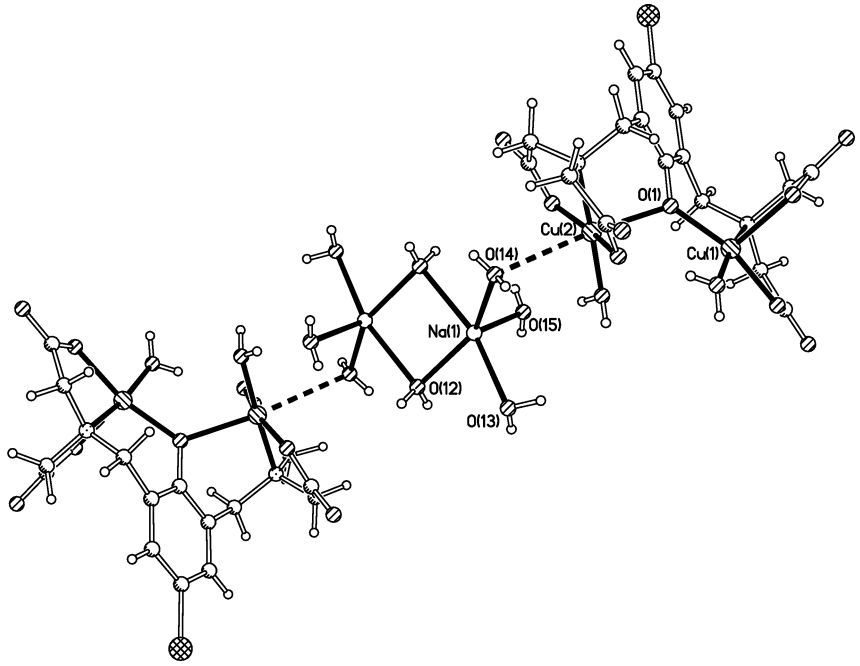

Figure 3. Two dinuclear units linked through the disodium countercationic unit in $[Cu_2(Cl\text{-}hxta)(H_2O)_3]_2[Na_2(\mu\text{-}H_2O)_2(H_2O)_6]\cdot 6H_2O$, **2**.

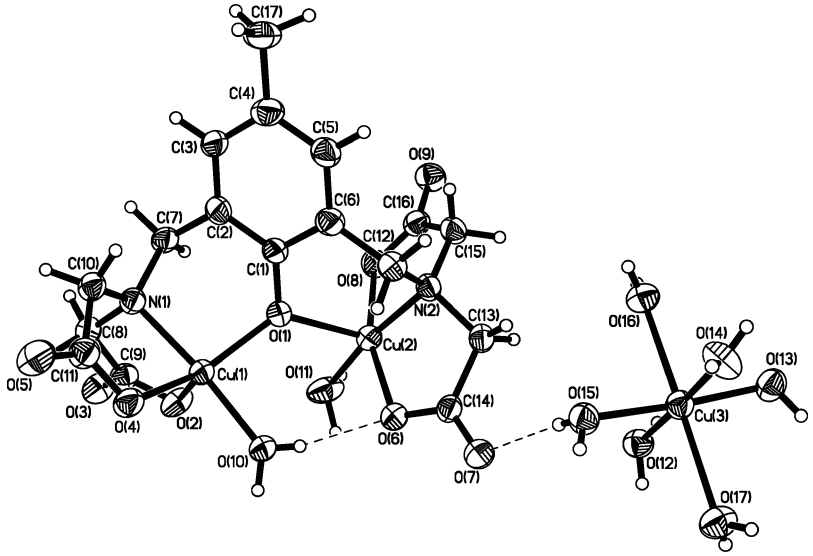

Figure 4. Structures of the complexes in $[Cu(H_2O)_6][Cu_2(Me\text{-}hxta)(H_2O)_2](NO_3)\cdot 2H_2O$, **3**.

from O(14), an aqua ligand from the $[Na_2(\mu\text{-}OH_2)_2(OH_2)_6]^{2+}$ countercation. This linkage results in a centrosymmetric structural unit in which two dinuclear copper(II) complexes are linked through the disodium cationic unit, as shown in Figure 3. The sodium centers in the cation are pentacoordinate, and are bridged by two aqua ligands.

In $[Cu(H_2O)_6][Cu_2(Me\text{-}hxta)(H_2O)_2](NO_3)\cdot 2H_2O$, **3**, the two copper(II) centers are again linked by an unsymmetrical phenoxy bridge; with Cu(1)−O(1) = 1.931(3) Å, Cu(2)−O(1) = 2.145(3) Å, the Cu(1)−O(1)−Cu(2) angle = 128.1(1)°, and Cu(1)···Cu(2) separation = 3.6675(7) Å (Figure 4). The environment about Cu(1) is square-based pyramidal. The apical site is occupied by the carboxylate oxygen O(4), while the square base is defined by the phenoxy oxygen O(1), carboxylate oxygen O(2), the amine nitrogen N(1), and an aqua ligand O(10). Cu(2) has a geometry similar to that seen in compounds **1** and **2**. Again, the equatorial plane is described by the amine nitrogen and two carboxylate oxygens from an arm of the ligand, together with an aqua ligand O(11), while O(1) is in an axial site. Figure 4 shows the structure of the dinuclear copper(II) complex together with the $[Cu(H_2O)_6]^{2+}$ countercation.

The nitrate ion balances the charge and is hydrogen bonded to an aqua ligand O(10) of the dinuclear complexes. The hydrogen-bonding network in **3** is more complicated than that in **1** and **2**. Each mononuclear $[Cu(H_2O)_6]^{2+}$ cation forms hydrogen bonds to seven different dinuclear complexes, while each dinuclear unit accepts hydrogen bonds from seven mononuclear complexes and in addition is hydrogen-bonded to a further dinuclear complex.

The dinuclear complexes $[Cu_2(R\text{-}hxtaH)(H_2O)_3]\cdot 3H_2O$ {R = Cl (**4**), CH_3 (**5**), and CH_3O (**6**)} have isomorphous crystal

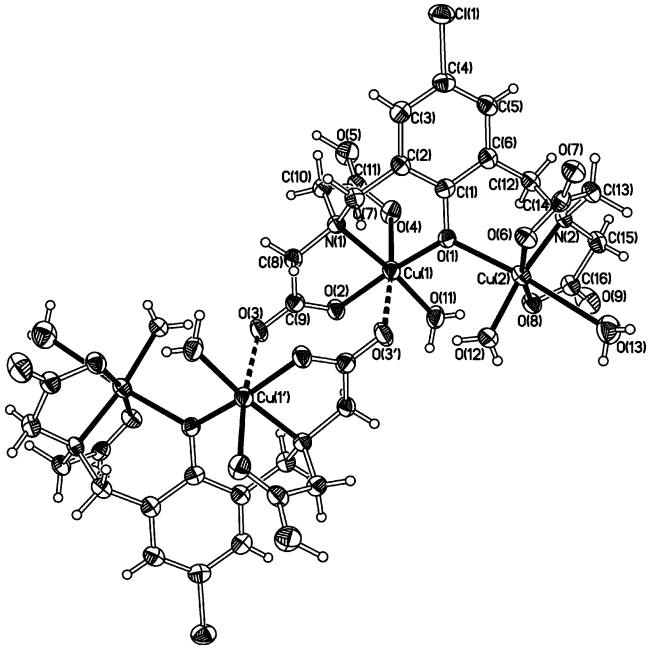

Figure 5. Dimer of dinuclear complexes $[Cu_2(Cl\text{-}hxtaH)(H_2O)_3]\cdot 3H_2O$, **4**.

structures, and the molecular structures are very similar. The structure of **4** is shown in Figure 5; the same atom numbering scheme is used for **5** and **6**.

Once again, O(1) mediates an unsymmetrical phenoxy bridge.The geometrical parameters for the bridges in the three complexes are listed in Table 4, where they are compared with those for **1** and **2**. The coordination geometry about Cu(2) is very similar to that in **2**, although in complexes **4**−**6** the aqua ligand O(13) now no longer has the possibility to coordinate to a countercationic unit. The geometry about Cu(1) is also similar to that in **1** and **2**, with O(4) in the axial position, but now the octahedral coordination is completed by O(3′), an outer carboxylate oxygen from the inversion-related molecule at $\{1 - x, 1 - y, 1 - z\}$. Although the Cu(1)−O(3′) distances are all slightly more than 3 Å (see Table 4), this interaction mediates (vide infra) a significant magnetic exchange interaction between the complexes, which can thus be described as a dimer of dinuclear complexes. Cu(1′) is not coplanar with Cu(1), O(2), O(3), C(10), and C(9), and the O(2)−C(10)−O(3)−Cu(1′) torsion angle is 102°, so that the bridge cannot be conveniently described as either *syn-anti* or *anti-anti*. Two views of the linkage are shown in Figure 6.

If the halide salts $CuX_2\cdot 6(H_2O)$ (X = Cl, Br) are used as starting material in place of $Cu(NO_3)_2\cdot 6(H_2O)$, the complexes $[Cu_2(CH_3O\text{-}hxtaH_2)(\mu\text{-}X)(CH_3OH)]\cdot 3CH_3OH$ (X = Cl (**7**) and Br (**8**)) are formed. These complexes crystallize isomorphously with very similar molecular structures; the structure of **7** is shown in Figure 7. The most notable feature

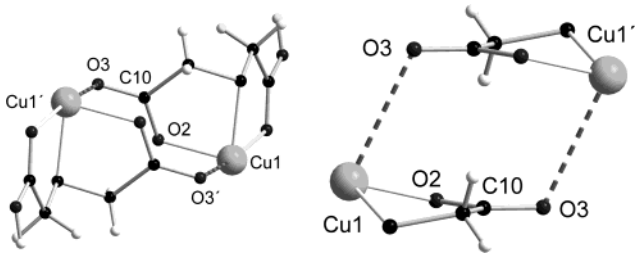

Figure 6. Views of the interdimer linkage for complexes **4**−**6**.

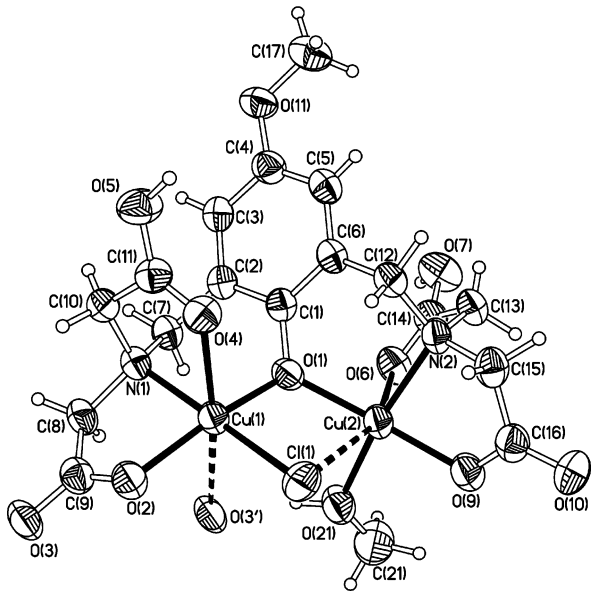

Figure 7. Dinuclear complex in $[Cu_2(CH_3O\text{-}hxtaH_2)(\mu\text{-}Cl)(CH_3OH)]\cdot 3CH_3OH$, **7**.

of the structures is the semi-bridging halide ligands coordinated to Cu(1) and, more weakly, to Cu(2), leading to an acute angle at the halide: Cu(1)−Cl(1) 2.2489(12) Å, Cu(1)−Br(1) 2.3915(5) Å, Cu(2)−Cl(1) 2.9345(14) Å, Cu(2)−Br(1) 3.0187(5) Å, Cu(1)−Cl(1)−Cu(2) 78.06(4)°, and Cu(1)−Br(1)−Cu(2) 75.18(1)°. In contrast to complexes **1**−**6**, the phenoxy bridges between Cu(1) and Cu(2) in **7** and **8** are nearly symmetrical (Table 4), with O(1) occupying equatorial positions in both coordination environments. The effect of the two bridges is to reduce the Cu(1)···Cu(2) distance relative to complexes **1**−**6**.

Both copper(II) centers have rather strongly distorted octahedral coordination geometries. The long Cu(2)−X(1) bond has the effect of making the halide and the carboxylate oxygen O(6) occupy the axial positions, while O(1), N(2), O(9), and the oxygen of a methanol ligand, O(21), describe the equatorial plane. The environment of Cu(1) is similar to that formed in **4**−**6**, with the halide ligands replacing the aqua ligand O(11) in the latter three complexes. Again, the octahedral coordination sphere is completed by O(3′), an

Table 4. Bond Lengths (Å) and Angles (deg) of Complexes **1**−**9**

	1	**2**	**3**	**4**	**5**	**6**	**7**	**8**	**9**
Cu(1)−O(1)	1.911(2)	1.917(2)	1.931(3)	1.904(3)	1.906(2)	1.893(2)	1.933(3)	1.930(2)	2.001(4)
O(1)−Cu(2)	2.174(2)	2.225(2)	2.145(3)	2.250(2)	2.231(2)	2.225(2)	1.939(3)	1.951(2)	2.005(4)
Cu(1)−O(1)−Cu(2)	130.9(1)	126.0(1)	128.1(1)	127.1(1)	127.9(1)	127.6(1)	117.3(1)	118.7(1)	116.3(2)
Cu(1)···Cu(2)	3.7172(6)	3.6933(4)	3.6675(7)	3.7329(5)	3.7201(6)	3.6982(7)	3.3071(7)	3.3375(5)	3.4039(10)
Cu(1)−O(3′)				3.084(2)	3.113(3)	3.046(3)	3.396(4)	3.378(3)	

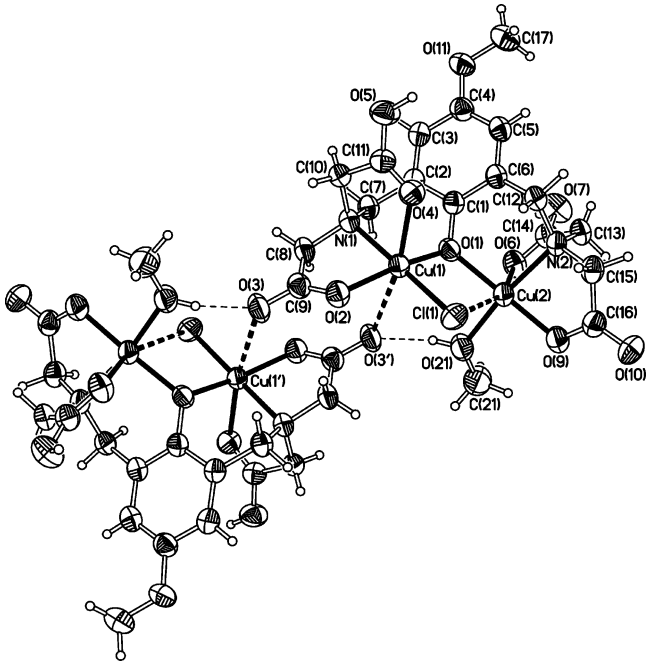

Figure 8. Dimer of dinuclear complexes in $[Cu_2(CH_3O\text{-}hxtaH_2)(\mu\text{-}Cl)(CH_3OH)]\cdot 3CH_3OH$, **7**.

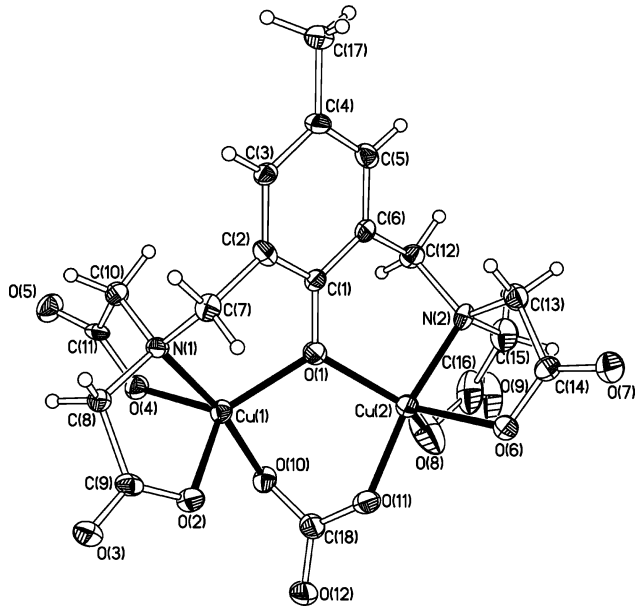

Figure 9. Structure of the $[Cu_2(\mu\text{-}CO_3)(Me\text{-}hxta)]^{3-}$ unit in **9**.

outer carboxylate oxygen from the inversion-related molecule at $\{1 - x, 1 - y, 1 - z\}$, resulting in a dimeric structure (Figure 8). The Cu(1)−O(3′) distances are, however, slightly longer than those in **4**−**6** (Table 4) but are supported by the hydrogen bond between O(21) of the methanol ligand and O(3′). Complexes **7** and **8** are neutral; the outer oxygens of the two axially coordinated carboxylate groups, O(5) and O(7), are protonated.

The use of KOH as base and prolonged reaction time results in the fixation of atmospheric CO_2 to give the carbonate-bridged complex $K_5Na(\mu\text{-}H_2O)_{10}[Cu_2(\mu\text{-}CO_3)(Me\text{-}hxta)]_2\cdot 4(H_2O)$, **9** (Figure 9). The identity of the bridging ligand was confirmed as carbonate from the microanalytical data, which were inconsistent with a nitrate ligand, from the strong band in the IR spectrum at 1344 cm^{-1}, and consideration of the charge balance, which requires a dianionic bridging ligand. We have recently observed the reaction of aqua ligands on oxo- and phenoxy-bridged polynuclear iron(III) complexes with atmospheric CO_2 to form bridging carbonate ligands,[30] and such fixation has also been observed in other copper(II) complexes.[31] However, although many bridging modes are known, it appears that the distorted *syn*, *syn*-bridging mode found in **8** has only once been previously characterized structurally in a copper(II) complex, even though it had been predicted as an antiferromagnetic exchange pathway.[30]

The phenoxy bridge between Cu(1) and Cu(2) is symmetrical and the geometry is similar to that in compounds **7** and **8**. Although the carbonato-bridge (Cu(1)−O(10) 1.930(4) Å, Cu(2)−O(11) 1.917(5) Å, C−O 1.251(8)−1.324(8) Å) is best categorized as *syn*, *syn*, it is twisted relative to the Cu(1)−O(1)−Cu(2) plane with a dihedral angle of 23°. This twist is in the opposite sense to that of the aromatic ring, so that the carbonate and phenoxy planes are close to orthogonal. In contrast to the other complexes reported here both Cu(1) and Cu(2) have trigonal-bipyramidal geometries, with the axial coordination involving a ligand nitrogen and a carbonate oxygen, while the equatorial planes are defined by O(1) and two carboxylate oxygens. The equatorial X−Cu−Y angles are in the range 108.0(2)−128.4(2)°.

The potassium and sodium countercations in **9** are linked by bridging water ligands to form irregular $\{K_5Na(OH_2)_{10}\}_n$ sheets in the crystal, parallel to {100}. The outer carbonate oxygen, O(12), is μ_3-coordinated to a triangle of three potassium cations, K(1), K(2), and K(3). Five of the eight carboxylate oxygens in the complex coordinate to potassium cations in the sheets. The dinuclear complexes are attached alternately above and below the $\{K_5Na(OH_2)_{10}\}_n$ sheets, so that the aromatic rings of their hxta ligands form parallel rows on each surface of the sheet (Figure 10). These rows on adjacent sheets intercalate with π-stacking of the ligands,[32,33] to build up the overall crystal structure.

Magnetic Properties. The magnetic measurements on these compounds show different types of interactions, reflecting the ligand bridging modes and the geometric parameters.

The temperature dependences of the χT product for **1**, **2**, and **3** are shown in Figure 11. At room temperature, the χT product is 0.89 emu·K·mol^{-1} (**1**), 0.88 emu·K·mol^{-1} (**2**), and 1.32 emu·K·mol^{-1} (**3**) in good agreement with what is expected for two and three isolated paramagnetic Cu(II) metal ions for **1**−**2** and **3**, respectively. Fitting of the experimental data using a simple dinuclear $S = {}^1/_2$ model[34] with an additional mean field approximation reproduce well the magnetic behavior with $J/k_B = +5.7$ K, $g = 2.17$, and $zJ' =$

(30) Schmitt, W.; Anson, C. E.; Sessoli, R.; Veen, M. v.; Powell, A. K. *J. Inorg. Biochem.* **2002**, *91*, 173−189.
(31) Youngme, S.; Chaichit, N.; Kongsaeree, P.; Albada, G. A. v.; Reedijk, J. *Inorg. Chim. Acta* **2001**, *324*, 232−240.
(32) Hunter, C. A.; Sanders, J. K. M. *J. Am. Chem. Soc.* **1990**, *112*, 5525−5534.
(33) Yang, G.; Yu, X.-L.; Chen, X.-M.; Ji, L.-N. *Cryst. Res. Technol.* **2000**, *35*, 993−1000.

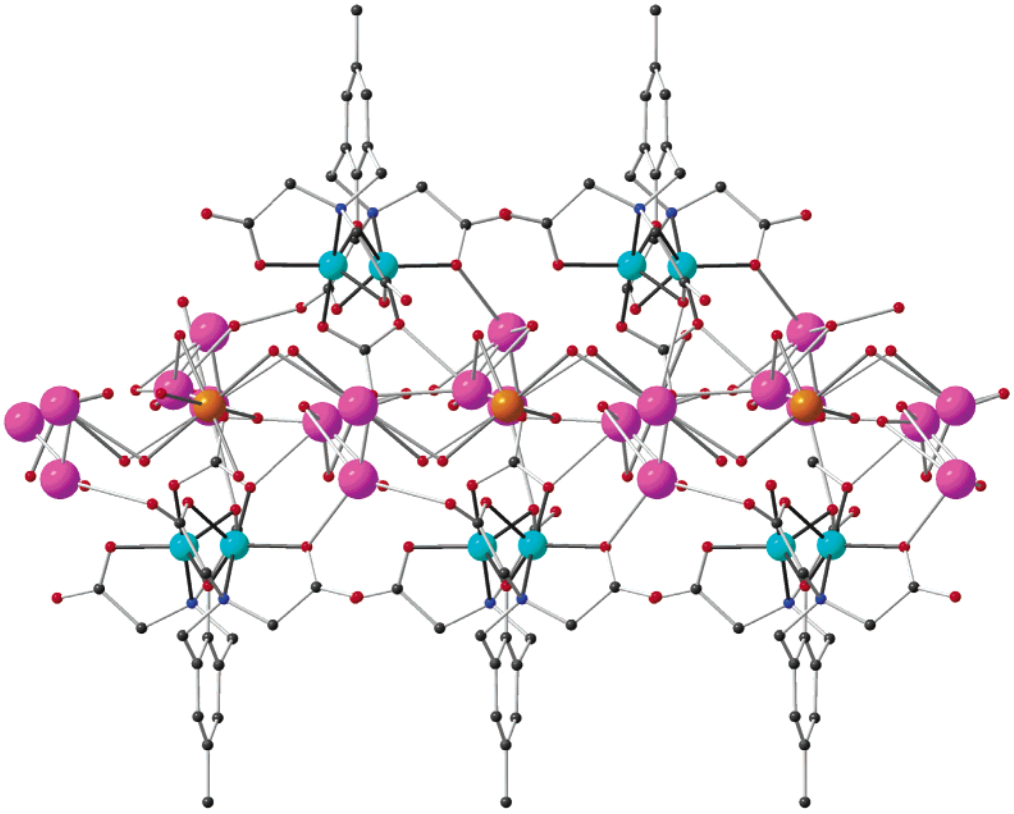

Figure 10. Coordination of the dicopper(II) complexes to the $\{K_5Na(OH_2)_{10}\}_n$ sheets in **9**, viewed along the crystal *c*-axis and showing the parallel orientation of the aromatic ligands (Cu, light blue; C, black; O, red; N, blue; K, purple; Na, orange).

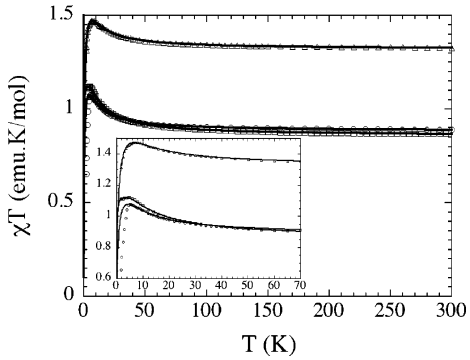

Figure 11. Temperature dependence of χT for **1** (○), **2** (□), and **3** (△) at 1000 G. The solid lines show the best fits obtained.

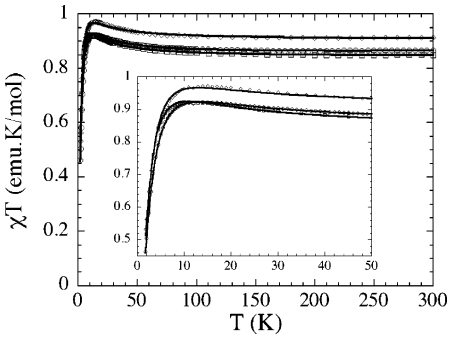

Figure 12. Temperature dependence of χT for **4** (○), **5** (◇), and **6** (□) at 1000 G. The solid lines show the best fits obtained.

-0.3 K (**1**) and $J/k_B = +8.1$ K, $g = 2.14$, and $zJ' = -0.04$ K (**2**). For **3**, the same model was used in addition to a Curie law to take into account the isolated $[Cu(H_2O)_6]^{2+}$ unit, the best set of parameters obtained is $J/k_B = +6.7$ K, $g = 2.16$, and $zJ' = -0.46$ K (**3**). The *g* values were confirmed by room-temperature EPR measurements which gave $g = 2.16$. The decrease of χT at low temperature is probably due to small antiferromagnetic interactions between $S = 1$ dinuclear complexes. The positive *J* value highlights the ferromagnetic nature of the interaction through the mono-phenoxy bridge.

In complexes **1** and **2**, Cu(1) has a *pseudo*-square pyramidal environment and Cu(2) is in a distorted octahedral geometry and thus will have $d_{x^2-y^2}$ as the highest d-orbital.

(34) Bleaney, B.; Bowers, K. D. *Proc. R. Soc. London* **1952**, A214. Note that we have considered the following Hamiltonian in this work: $H = -2J(S_1S_2)$

Scheme 2. Schematic Representation of the Orbital Orientation in **1**−**6**

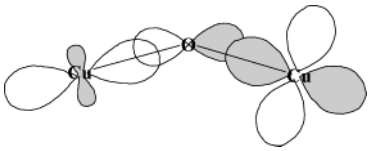

The bridging phenoxy-oxygen atom is in an axial position for Cu(1) and in an equatorial position relative to Cu(2). Thus it has bonding interactions with the d_{z^2} and $d_{x^2-y^2}$ orbitals of Cu(1) and Cu(2) respectively, as shown in Scheme 2. Consequently the two $d_{x^2-y^2}$ orbitals are orthogonal, so the oxygen atom does not mediate an interaction between them, and only weak ferromagnetic interactions are observed.

The χT versus *T* plots for **4**−**6** at 1000 G are shown in Figure 12. At high temperature, between 100 and 300 K, the χT product remains essentially constant 0.867 (**4**), 0.914 (**5**),

Scheme 3

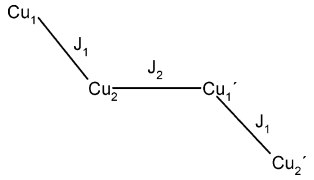

and 0.850 emu·K·mol^{-1} (**6**). Upon cooling, the χT product increases up to 15 K to reach a value of 0.942 (**4**), 0.972 (**5**), and 0.923 emu·K·mol^{-1} (**6**). This behavior reveals the presence of dominating ferromagnetic interactions between copper(II) centers. Below 15 K, the χT product decreases continuously to reach a value of respectively 0.462, 0.532, and 0.617 emu·K·mol^{-1} for **4**−**6** at 1.83 K. This behavior is the result of weak anti-ferromagnetic interactions between copper binuclear units.

Considering the molecular structure of compounds **4**−**6**, the Hamiltonian[35] for a tetramer, $H = -2J_1(S_1S_2 + S_3S_4) - 2J_2S_3S_4$, was applied which corresponds to the system shown in Scheme 3 in which J_1 is the exchange constant between two copper ions in the dinuclear complex and J_2 is the coupling constant between two copper ions linked through *syn(ax)*−*anti(eq)* carboxylate bridges. This Hamiltonian can be solved exactly and the experimental data were fitted to this expression

$$\chi = \frac{Ng^2{\mu_B}^2}{k_BT} \times \left[10\exp\left(\frac{-E_1}{k_BT}\right) + 2\exp\left(\frac{-E_2}{k_BT}\right) + 2\exp\left(\frac{-E_3}{k_BT}\right) + 2\exp\left(\frac{-E_4}{k_BT}\right)\right]/Z$$

$$Z = 5\exp\left(\frac{-E_1}{k_BT}\right) + 3\left[\exp\left(\frac{-E_2}{k_BT}\right) + \exp\left(\frac{-E_3}{k_BT}\right) + \exp\left(\frac{-E_4}{k_BT}\right) + \exp\left(\frac{-E_5}{k_BT}\right) + \exp\left(\frac{-E_6}{k_BT}\right)\right]$$

where

$$E_1 = -J_1 - \frac{1}{2}J_2$$

$$E_2 = J_1 - \frac{1}{2}J_2$$

$$E_3 = \frac{1}{2}J_2 + ({J_1}^2 + {J_2}^2)^{1/2}$$

$$E_4 = \frac{1}{2}J_2 - ({J_1}^2 + {J_2}^2)^{1/2}$$

$$E_5 = J_1 + \frac{1}{2}J_2 + (4{J_1}^2 - 2J_1J_2 + {J_2}^2)^{1/2}$$

$$E_6 = J_1 + \frac{1}{2}J_2 - (4{J_1}^2 - 2J_1J_2 + {J_2}^2)^{1/2}$$

The magnetic susceptibility data obtained by a least-squares method summarized in Table 5 show a dominant ferromagnetic interaction between Cu(1) and Cu(2) through the mono-phenoxy bridge. In compounds **4**−**6**, Cu(1) and Cu(2) have distorted octahedral geometries and thus will have $d_{x^2-y^2}$ ground states. The bridging phenoxy-oxygen atom is in an axial position for Cu(1) and in equatorial position relative to Cu(2). Thus d_{z^2} and $d_{x^2-y^2}$ orbitals of Cu(1) and Cu(2), respectively, interact as shown in Scheme 2. The two $d_{x^2-y^2}$ orbitals are orthogonal, so the oxygen atom does not mediate an interaction between the ground states and so weak ferromagnetic interactions are observed. There is also a weak anti-ferromagnetic interaction between these two binuclear units through *syn(ax)*−*anti(eq)* carboxylate bridges.

Table 5. Magnetic Susceptibility Parameters of **4**−**6**

	4	**5**	**6**
J_1/k_B (K)	+6.8	+5.4	+6.5
J_2/k_B (K)	−3.4	−3.3	−2.8
g_{squid}	2.13	2.19	2.11
g_{EPR}	2.137	2.166	2.140

In complexes **1**−**6**, a relationship between the structural and magnetic properties is observed. In Table 6 selected geometric parameters are listed together with those for three other previously reported complexes with *ax*−*eq* phenoxo bridges, $[Cu_2(Me\text{-}bpmp)(OH_2)_2](ClO_4)_3\cdot 4H_2O$,[11] **A**, $[Cu_2(py_3\text{-}asym)(OH_2)_{1.5}(NO_3)_2](NO_3)$,[12] **B**, and $[Cu_2(Me\text{-}bbmp)(OH_2)_2](ClO_4)\cdot 3H_2O$,[13,14] **C**. Data for two further complexes with *ax*−*ax* bridges, $[Cu_2(Me\text{-}bimp)(OH_2)_2](ClO_4)_3\cdot 3H_2O$,[10] **D**, and $[Cu_2(Me\text{-}bpmp)Cl_2](ClO_4)$,[9] **E**, are also given for comparative purposes. The ligands Me-bpmp$^-$, Me-bimp$^-$, and Me-bbmp$^-$ are related to Me-hxta^{5-} in that the carboxylate groups of the latter ligand have been replaced by 2-pyridyl, 2-imidazolyl, or 2-benzimidazoloyl groups, respectively. The py$_3$asym$^-$ ligand has three pyridyl-bearing arms. In these compounds the relationship between the coupling constant and the angle of the bridge is *quasi* linear. The data of our compounds along with the compounds **A**, **B**, and **C** can be fitted using the linear function $J = 66.54 - 0.47\alpha$ as shown in Figure 13. The J value increases with decreasing bridging angle. Qualitatively good agreement between α and the magnetic interaction J in this series of compounds is observed because the other geometric parameters are rather similar, leaving α as the only significant variable. While the Cu−O−Cu angle is unlikely to be the only parameter which influences the magnetic interaction, it appears from this analysis to be the most pertinent one. Since there is a degree of variation in the ligands and the coordination spheres of the copper centers in the complexes reported here and in the literature complexes, it would appear that the relationship between J and α is reasonably robust, and should have predictive value.

The two related complexes with *ax*−*ax* bridges, **D** and **E**, also give points shown on the graph in broad agreement with the geometrical relationship. However, since they both have $J \approx 0$, it might be wise to wait for data for such a complex with a rather different bridging angle α before assuming that the relationship presented here also applies to mono-bridged dinuclear complexes with this orbital geometry. It is worth noting that for the other possible symmetric bridge, *eq*−*eq*, in which the $d_{x^2-y^2}$ orbitals on both coppers are involved in

(35) Escuer, A.; Kumar, S. B.; Font-Bardia, M.; Solans, K.; Vicente, R. *Inorg. Chim. Acta* **1999**, *286*, 62−66.

Table 6. Selected Geometric Parameters for Compounds **1**−**6** and Other Previously Reported Compounds

compound	J/k_B (K)	Cu(1)−O(1)−Cu(2)	Cu(1)···Cu(2)	Cu(1)−O(1)	Cu(2)−O(1)
		ax−*eq* bridge			
1	+5.7	130.9	3.717	1.911	2.174
2	+8.1	126.0	3.693	1.917	2.285
3	+6.7	128.1	3.667	1.931	2.145
4	+6.8	127.0	3.721	1.906	2.250
5	+5.4	127.9	3.720	1.906	2.231
6	+6.5	127.6	3.698	1.893	2.208
A Torreli[a]	0.0	142.0	4.139	2.005	2.189
B Koval[b]	+3.3	133.5	3.900	1.934	2.307
C Berends[c]	+6.1	128.4	3.875	1.920	2.280
		ax−*ax* bridge			
D Oberhausen[d]	+0.2	142.9	4.090	2.156	2.156
E Nishida[e]	0.0	140.2	4.13	2.16	2.23

[a] Ref 11. [b] Ref 12. [c] Refs 13 and 14. [d] Ref 10. [e] Ref 9.

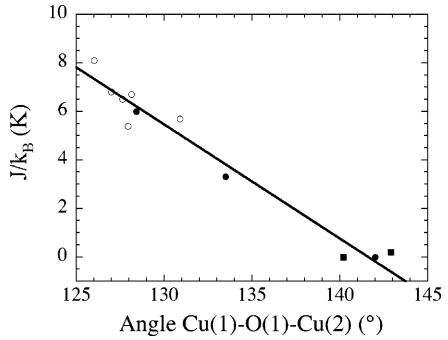

Figure 13. Plot of J/k_B versus the angle Cu(1)−O(1)−Cu(2) (α). Open circles represent data for *ax*−*eq* bridges from this work, and filled circles represent data from refs 11−14 which have been fit using the relationship given in the text. Filled squares show where the parameters lie for the *ax*−*ax* linked compounds from refs 9 and 10 for comparison.

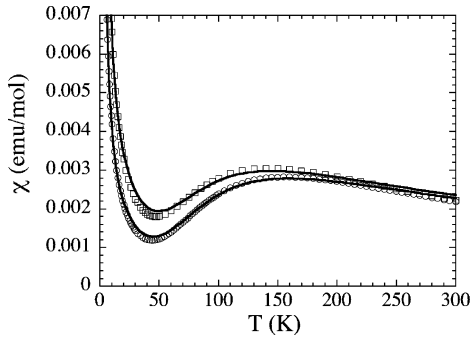

Figure 14. Temperature dependence of χ for **7** (□) and **8** (○) at 1000 G. The solid lines show the best fits obtained.

the bridge, the relationship clearly does not hold. For the only example of such a complex so far reported, Na[Cu_2-(Me-hxta)$(pyr)_2$]·$1^1/_2$(dioxane), α = 123.7°, while the complex is strongly antiferromagnetically coupled, with J = −121 K.[21]

The magnetic properties of **7** and **8** are shown in Figure 14 as the temperature dependence of χ over the range 1.8−300 K and are typical for anti-ferromagnetic coupled systems.

Despite the structural analysis showing that these dinuclear complexes are linked via *syn(ax)*−*anti(eq)* carboxylate bridges to another dinuclear complex (Figure 8) as for compounds **4**−**6**, **7** and **8** can be analyzed using the classical Bleaney−Bowers equation[31] for a pair of spin = $^1/_2$. The expected weak ferromagnetic interactions between dinuclear complexes mediated by *syn(ax)*−*anti(eq)* carboxylate ligands

Table 7. Magnetic Susceptibility Parameters for **7** and **8**

	7	**8**
J_1/k_B (K)	−123	−131
g_{squid}	2.11	2.14
g_{EPR}	2.167	2.150

Scheme 4. Orbital Representation of **7** and **8**

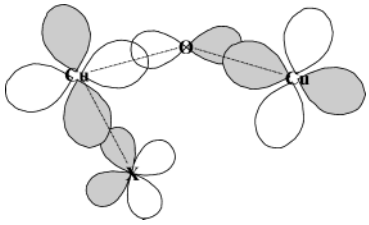

are negligible and cannot be estimated due to the strong antiferromagnetic interactions within the dinuclear complex which lead to a singlet ground state of the dimer and the g and J values obtained from the least-squares fittings of the experimental data are summarized in Table 7.

In compounds **7** and **8**, Cu(1) and Cu(2) both have distorted octahedral geometries and in each case the unpaired electron occupies a $d_{x^2-y^2}$ orbital as shown in Scheme 4. The bridging phenoxy oxygen is in an equatorial position for both copper atoms, allowing strong overlap between the antisymmetric combination of the two $d_{x^2-y^2}$ orbitals of the copper centers and the oxygen p_x orbital. Given the relatively large Cu−O−Cu angle, interaction of the symmetric combination with the oxygen p_z orbital will be much smaller, resulting in a large splitting of the symmetric and antisymmetric combinations of $d_{x^2-y^2}$, and leading to the observed antiferromagnetic coupling in compounds **7** and **8**.

Previously reported[36−38] Cu(II) (*ax*−*ax*) mono-chloride bridged complexes show magnetic interactions with a trend from moderate antiferromagnetic[37] (−14 K) to moderate ferromagnetic[38] (+12 K) on decreasing the angle of the bridge from approximately linear to 124°. However, in complexes **7** and **8**, the Cu−X−Cu angle is much smaller, indeed acute (75° (**7**) and 78° (**8**)) and extrapolation of the

(36) Du, M.; Guo, Y. M.; Bu, X. M.; Ribas, J.; Monfort, M. *New J. Chem.* **2002**, *26*, 939−945.
(37) Zhu, H. L.; Zheng, L. M.; Fu, D. G.; Hang, P.; Bu, W. M.; Tang, W. X. *Inorg. Chim. Acta* **1999**, *287*, 52.
(38) Decurtins, S.; Schmalle, H.; Schneuwly, P.; Zheng, L. M.; Ensling, J.; Hauser, A. *Inorg. Chem.* **1995**, *34*, 5501.

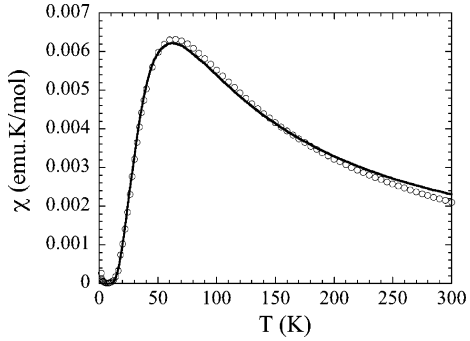

Figure 15. Temperature dependence of χ for **9** (○) at 1000 G. The solid line shows the best fit.

above trend may not be advisable. The semi-bridging halide is unlikely to be a significant exchange pathway in its own right, since it does not interact with a magnetic d orbital on either copper center, but it does have a very significant effect on the magnetic properties of **7** and **8** in that it forces the coordination geometries about both coppers to be ideally set up for strong antiferromagnetic exchange. This is consistent with the complex $Na[Cu_2(Me\text{-}hxta)(pyr)_2]\cdot 1^1/_2(dioxane)$, which has an *eq*−*eq* phenoxy-bridge unsupported by any semi-bridging ligand with a geometry similar to that in **7** and **8**, with Cu−O = 1.999 and 2.005 Å and $\alpha = 123.7°$, and shows a coupling constant $J = -121$ K that is close to those in **7** and **8**.[21] By contrast, all the previously reported dinuclear copper(II) complexes with phenoxy and halide bridges have essentially symmetrical halide bridges with both bridging atoms in equatorial positions on each of the copper centers and well placed to interact with the two $d_{x^2-y^2}$ orbitals.[9,39−43] They show antiferromagnetic coupling similar to or stronger than that in **7** and **8**, but the presence of two magnetic bridges and generally a significantly smaller Cu−O−Cu angle makes direct comparison meaningless.

The temperature dependence of χ for compound **9** is shown in Figure 15 and can be interpreted in terms of the presence of a strong antiferromagnetic interaction between Cu(1) and Cu(2). This compound can again be analyzed with the classical equation of Bleaney and Bowers.[34] The best fit obtained with the experimental data gives $J/k_B = -50$ K, $g = 2.15$.

The geometry around each copper in complex **9** is pseudo-trigonal bipyramidal, which leads to a d_{z^2} ground state. The principal lobes are oriented along the axial direction of the trigonal bipyramid toward the bridging carbonate, with the d_{z^2} orbitals of each copper ion interacting similarly with the bridging carbonate orbitals. We are unaware of any structurally characterized copper(II) complexes with bridging *syn*, *syn*−carbonato ligands. A dinuclear copper(II) complex with a *syn*, *syn*−bridging hydrogencarbonato ligand has been reported.[44] However, the geometries about the copper centers

Scheme 5. Antisymmetrical Orbital Combination (left) and Symmetrical Orbital Combination (right) of Complex **9**

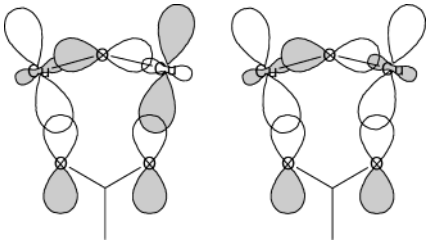

in this complex are square-based pyramidal with the hydrogencarbonato oxygens in equatorial sites, in contrast to the trigonal-bipyramidal geometries for **9**, consequently the magnetic properties (ferromagnetic coupling with $J = +26.0$ K) are very different from those of **9**. It is, however, possible to compare the magnetic behavior in **9** with related acetato-bridged complexes. Where such complexes have distorted octahedral or square-pyramidal coordination spheres around both coppers, the interaction is moderately antiferromagnetic (−25 and −32 K).[45,46] With one copper square-pyramidal and the other trigonal-bipyramidal, or with both coppers having geometries intermediate between square-pyramidal and trigonal-bipyramidal, the coupling is negligible.[47,48] When both coppers have a trigonal-bipyramidal geometry similar to that in **9**, however, moderate ferromagnetic coupling (+11 and +12 K) is observed.[49,50] This has been attributed to the noncomplementary interactions between the symmetric and antisymmetric combinations of the two d_{z^2} orbitals with the phenoxy p_x orbital and with the acetate HOMO, respectively, which result in a small separation between the two magnetic orbitals (Scheme 5).[51] In contrast to the last two complexes, **9** shows significant antiferromagnetic coupling. The 4*e*′ HOMO of the isolated carbonate anion is expected to split under the C_{2V} symmetry of the complex to give two orbitals of similar energy, one of which will interact with the symmetric combination of the d_{z^2} orbitals, the other of which will interact with the antisymmetric combination. This additional interaction with the antisymmetric combination compared to the acetate situation is likely to result in a larger splitting between the two magnetic orbitals, which would then make antiferromagnetic coupling more likely.

Conclusions and Outlook

We have shown how the magnetic coupling in a series of related Cu(II) dinuclear magnetic bricks can be correlated to

(39) Benzekri, A.; Dubourdeaux, P.; Latour, J. M.; Laugier, J.; Rey, P. *Inorg. Chem.* **1988**, *27*, 3710−3716.
(40) O'Connor, C. J.; Firmin, D.; Pant, A. K.; Babu, B. B.; Stevens, E. D. *Inorg. Chem.* **1986**, *25*, 2300−2307.
(41) Butcher, R. J.; O'Connor, C. J.; Sinn, E. *Inorg. Chem.* **1981**, *20*, 537.
(42) Eduok, E. E.; O'Connor, C. J. *Inorg. Chim. Acta* **1984**, *88*, 229−233.
(43) Karlin, K. D.; Farooq, A.; Hayes, J. C.; Cohen, B. I.; Rowe, T. M.; Sinn, E.; Zubieta, J. *Inorg. Chem.* **1987**, *26*, 1271−1280.
(44) Nishida, Y.; Yatani, A.; Nakao, Y.; Taka, J.-I.; Kashino, S.; Mori, W.; Suzuki, S. *Chem. Lett.* **1999**, 135−136.
(45) Murthy, N. N.; Karlin, K. D.; Bertini, I.; Luchinat, C. *J. Am. Chem. Soc.* **1997**, *119*, 2156−2162.
(46) Neves, A.; Rossi, L. M.; Vencato, I.; Drago, V.; Haase, W.; Werner, R. *Inorg. Chim. Acta* **1998**, *281*, 111−115.
(47) Cai, L. W.; Xie, H.; Mahmoud, Y.; Han, D. J.; Wink, S. L.; O'Connor, C. J. *Inorg. Chim. Acta* **1997**, 231−245.
(48) Sorell, T. N.; O'Connor, C. J.; Anderson, O. P.; Reibenspies, J. H. *J. Am. Chem. Soc.* **1985**, *107*, 4199−4206.
(49) Nie, H.; Aubin, S. M. J.; Mashuta, M. S.; Porter, R. A.; Richardson, J. F.; Hendrickson, D. N.; Buchanan, R. M. *Inorg. Chem.* **1996**, *35*, 3325−3334.
(50) McKee, V.; Zvagulis, M.; Dagdigian, J. V.; Patch, M. G.; Reed, C. A. *J. Am. Chem. Soc.* **1984**, *106*, 4765−4772.
(51) Hay, P. J.; Thibeault, J. C.; Hoffmann, R. *J. Am. Chem. Soc.* **1975**, *97*, 4884−4489.

the structural parameters in a relatively straightforward way. As we have shown in previous work,[2] mixing signs and magnitudes of magnetic coupling in molecular motifs forming ordered solids can result in materials with several magnetic phases which could find uses in thermally switched applications. The bricks we have discussed here could also be organized into arrays, for example, via carboxylate bridging,[3,52] which would allow for a variety of coupling possibilities thus suggesting a future direction for producing new materials based on these motifs.

(52) Murugesu, M.; Anson, C. E.; Powell, A. K. *Chem. Commun.* **2002**, 1054−1055.

Acknowledgment. We thank P. King, M. Murugesu, and X. Legoff for technical help on collecting magnetic data on some of the compounds. We acknowledge the ESF "Molecular Magnets" program for funding short scientific stays of R.C. and S.L. R.C. thanks also the Conseil Régional d'Aquitaine and the CNRS and A.K.P. thanks the DFG for financial support.

Supporting Information Available: X-ray crystallographic files in CIF format and EPR spectra used to derive the *g*-values (PDF). This material is available free of charge via the Internet at http://pubs.acs.org.

IC035333M